Polymer Chemistry

ROYAL SOCIETY OF CHEMISTRY

REVIEW

View Article Online
View Journal | View Issue

Cite this: *Polym. Chem.*, 2023, **14**, 2145

Photopolymerization shrinkage: strategies for reduction, measurement methods and future insights

Monika Topa-Skwarczyńska *[a,c] and Joanna Ortyl *[a,b,c]

Herein, a review of the literature on polymerization shrinkage occurring in dental composites was presented. In particular, methods of reducing polymerization shrinkage in dental composites by using alternative monomers and photoinitiators were described. Thus, new alternative materials for use in polymerization processes to obtain composites with limited polymerization shrinkage were presented. The effects of time and type of setting, as well as the type and amount of inorganic fillings, on the value of polymerization shrinkage were also discussed. It was explained why standard dental composites exhibit high polymerization shrinkage and why volume shrinkage and shrinkage stress are key factors in determining the quality of polymeric materials for dental applications. Traditional and new methods for testing polymerization shrinkage of composites were also presented. The advantages and disadvantages of methods for measuring polymerization shrinkage in dental composites were also presented and future insights were highlighted.

Received 12th March 2023,
Accepted 27th March 2023

DOI: 10.1039/d3py00261f

rsc.li/polymers

1. Introduction

In recent years, particular focus has on finding new solutions for photopolymerization processes has been placed.[1–10] This research involves both the search for new initiator systems,[7,11–14] fluorescent sensors[10,15–17] to monitor the progress of the polymerization process, new resins,[18,19] and new applications.[17,20,21] In recent years, significant progress in the development of photo-curable dental composites obtained by photopolymerization process was contributed. The research concerned both new photoinitiators,[22–26] new monomers[19,27–33] for dental fillings. Nevertheless, manufacturers of dental fillings are still looking for composites with reduced polymerization shrinkage and reduced shrinkage stress. An ideal dental composite would experience zero or at least little shrinkage during setting. Zero shrinkage would ensure that the material would remain physically adherent to the tooth surface without changing dimensions afterwards if the material itself did not absorb water over time. However, the typical dimethacrylate monomers used in commercial dental composites absorb water,[34] and therefore it may generally be advantageous for some composite shrinkage to occur, at least those based on the monomers, which will then be compensated by delayed expansion during service. In any event, the production of composites with low shrinkage, often described as less than 1.0% by volume, has been a manufacturers target for many years. However, the real problem with cure shrinkage, which is inevitable due to the nature of the polymerization of acrylate monomers to reduce intermolecular size and free volume, is the internal stress generated in the material.[35–37] This stress is a result of the restriction of the free contraction of the polymer and is dependent on many factors including the size and nature of the monomers, the stiffness of the material during polymerization, the rate of reaction, and the external constraints imposed by tooth bonding.

This article presents the main strategies for reducing polymerization shrinkage in dental composites with an emphasis on the use of appropriate photoinitiators and monomers as well as new and standard methods of measuring polymerization shrinkage. In this article, we have also presented future insights in the design of resins with limited polymerization shrinkage (Fig. 1).

2. General information about polymerization shrinkage

Volumetric/polymerization shrinkage and shrinkage stress are often used interchangeably, but they have two different definitions.

Resin composites based on acrylate monomers undergo a volumetric shrinkage of 2–14% after setting, which creates

[a]Department of Biotechnology and Physical Chemistry, Faculty of Chemical Engineering and Technology, Cracow University of Technology, Warszawska 24, 31-155 Cracow, Poland. E-mail: monika.topa@doktorant.pk.edu.pl, jortyl@pk.edu.pl
[b]Photo HiTech Ltd, Bobrzyńskiego 14, 30-348 Cracow, Poland
[c]Photo4Chem Ltd, Lea 114/416A-B, 31-133 Cracow, Poland

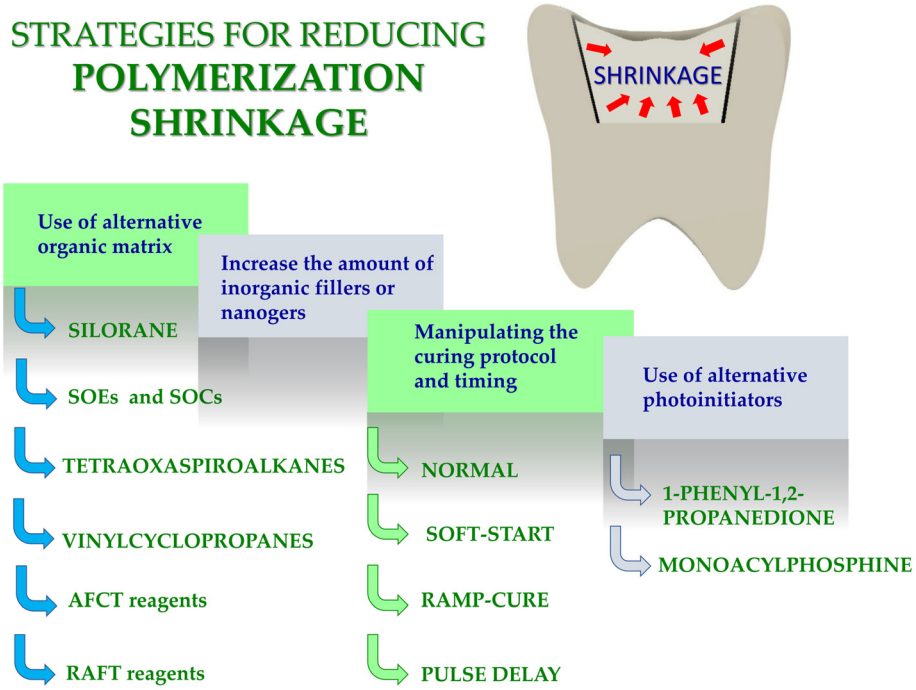

Fig. 1 Scheme illustrating strategies for reducing polymerization shrinkage.

5–15 MPa contraction stresses between the dental composite and the tooth, straining the interface, leading to detachment, microcracks and bending of the nodule.[38] The factor is not the polymerization shrinkage itself, but rather the stress generated by the reconstruction of the tooth interface, while the material shrinks in a confined environment such as tooth cavities or root canals.[39]

The greater the volumetric shrinkage, the greater the shrinkage stress for a comparable modulus of elasticity. The development of shrinkage stresses depends on the volumetric shrinkage strain and the stiffness of the composite at shrinkage; even low shrink composites can exhibit high stresses when they have a high modulus of elasticity.

It is usually recommended to apply the composite 2 mm in steps and polymerize each increment independently to ensure full depth of cure and reduce the net effect of polymerization shrinkage.[40–42] It is assumed that the net shrinkage stress is lower because the smaller volume of the composite may shrink before subsequent additions. On the other hand, Versluis *et al.* showed that incremental application in combination with the fixed bond with the tooth increased the deformation of the reconstructed tooth, and thus the stress level within the tooth restoration complex.[43] Both shrinkage stress[44] and volumetric/polymerization shrinkage of dental composites is the subject of much research.

Most popular organic matrixes designated for obtaining dental composites *via* photopolymerization are (meth)acrylate-monomers (RCB – resin based composites) characterized by high reactivity.[18]

Typically, monomers that polymerize according to the radical mechanism are 2,2-bis[4-(2-hydroxy-3-methacryloxypropyl)phenyl]propane (Bis-GMA), ethoxylated Bis-GMA (EBPDMA) and 1,6-bis-[2-methacryloxycarbonylamino]-2,4,4-trimethylhexane (UDMA), dodecanedioldimethacrylate (D3MA) or triethyleneglycolmethacrylate (TEGDMA) (Fig. 2). The choice of organic matrix is of considerable importance in the production of dental fillings. Such parameters as reactivity, viscosity, water absorption, swelling and, most importantly, polymerization shrinkage depend on its choice. Unfortunately, the polymerization shrinkage of dental composites that polymerize according to the radical mechanism ranges from 2 to as much as 14%.[45] The polymerization shrinkage of small-molecule monomers is more pronounced compared to macromolecular monomers; however, macromolecular monomers are very viscous (Table 1). For these reasons, polymerization shrinkage is dictated by the complex interplay of resin viscosity, polymerization rate, conversion rate and network structure evolution. Each of these parameters is important, and all of the listed parameters depend on each other, so they must be considered as a whole.

Moreover, because of the non-homogeneous network architecture created during the free-radical photopolymerization process, the final materials to be brittle, and the resulting shrinkage stress might lead to delamination, deformation, or mechanical failure of the final composites materials. The observed shrinkage stress evolves throughout the polymerization procedure as the applied formulation transitions from a liquid to a solid form (*i.e.* gel point) and is built up during vitrification until the ultimate conversion is attained. Prior to free-radical photopolymerization, the monomers are separated by van der Waal's distance (about 3.4 Å). The shrinkage stress that occurs during gelation is caused in part by the creation of covalent connections between the corresponding monomers,

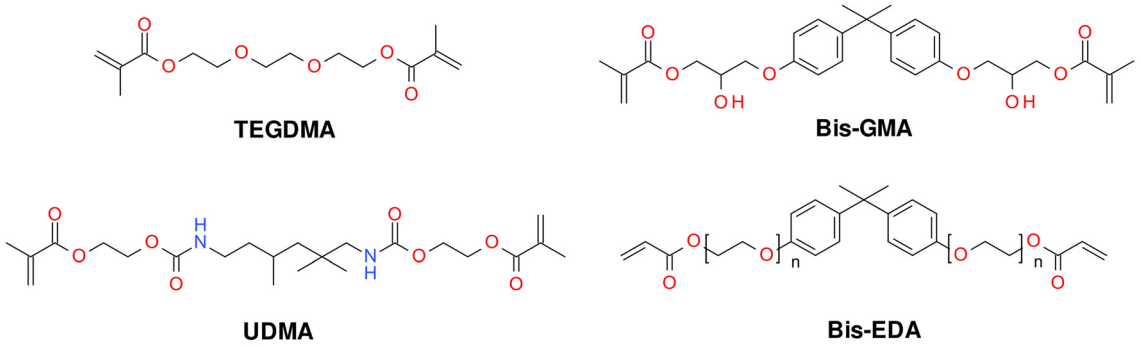

Fig. 2 Examples of monomers used in commercial dental composites based on free-radical photopolymerization mechanism.

Table 1 Properties of standard monomers used in production of dental composites

Monomer	Molecular weight [g mol^{-1}]	ρ_{mon} [a] [g cm^{-3}]	ρ_{pol} [b] [g cm^{-3}]	ΔV_p [%]	Viscosity [mPa s]
TEGDMA	286	1.072	1.250	−14.3	100
UDMA	470	1.110	1.190	−6.7	5000–10 000
Bis-GMA	512	1.151	1.226	−6.1	500 000–800 000

[a] ρ_{mon} – density of monomer. [b] ρ_{pol} – density of polymer.

where the disclosing distance is only 1.5 Å.[39] One of the key problems of contemporary methacrylates resin-based dental composites is incomplete free-radical photopolymerization, volumetric shrinkage, and stress. Attempts to boost double-bond conversion have often exacerbated polymerization shrinkage and polymerization stress. Furthermore, there is rising concern regarding the safe clinical use of these compounds due to their toxic effects, oral biodegradation,[46] and allergic effects.[47] Luo *et al.* proposed an alternative monomer urethane dimethacrylate monomer, which has lower polymerization shrinkage compared to BisGMA and UDMA (Fig. 3).[133]

On the other hand, Carlos E. Cuevas-Suárez proposed allyl carbonate monomer (BPhADAC, Fig. 4) as alternative to TEGDMA. They showed that the introduction of BPhADAC monomer in place of TEGDMA reduces polymerization shrinkage from 5.37% to 4.48%.[135]

Volumetric shrinkage and shrinkage stress are key factors in determining the quality of polymeric materials for dental applications. The shrinkage stress found in standard dental composites can even exceed the tensile strength of the enamel and cause stress cracks and fractures in the enamel along the interface. Such shrinkage stresses could also cause deformation of the surrounding tooth structure when the composite-tooth bond is strong, predisposing the tooth to fracture.[49–51]

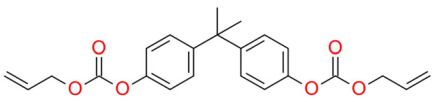

Fig. 4 Structure of BPhADAC monomer.

Moreover this stress may produce defects in the composite-tooth bond, leading to bond failure, micro leakage, postoperative sensitivity, and recurrent caries. Reconstruction failures in the form of hypersensitivity, pulpitis and secondary caries may occur.[50–52] In addition, the polymerization shrinkage causes mechanical stresses in the dental composites, which significantly reduces its mechanical strength.

3. Strategies for reducing polymerization shrinkage in dental composites

Many strategies to reduce polymerization shrinkage in dental composites have been developed. In particular, the polymerization shrinkage depends on:

(a) time and type of setting;

(b) type and quantity of inorganic fillings;

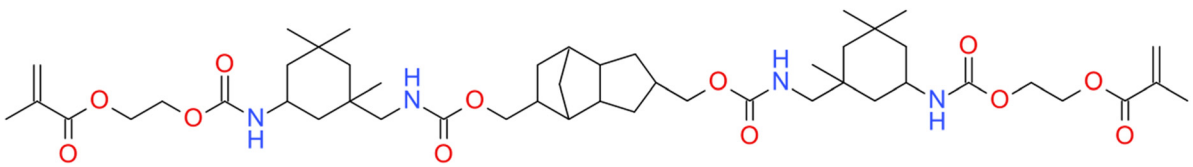

Fig. 3 Structure of urethane dimethacrylate monomer.

(c) type of organic matrix;
(d) type of photoinitiator.

Therefore, in recent years, scientists are working on strategies to reduce shrinkage stress. Below, the primary strategies for reducing the polymerization shrinkage of dental composites are presented (Fig. 1).

3.1. Time and type of setting – alternative curing methods

As the composite is polymerized under various illumination circumstances, shrinkage stress varies. Several research have shown that the modification of irradiance during the photoactivation process affects the shrinkage stress modulus.[39] In order to minimize the effects of polymerization shrinkage, alternative light activation protocols have been recommended.[53,54] Fig. 5 presents the different dental light-curing modes.[55] Soft-start techniques have been widely researched. In this type of photoactivation, low light intensity is used for a few seconds at the beginning, followed by a gradual increase in light intensity. This approach is recommended to reduce shrinkage stress, while maintaining a high degree of monomer-to-polymer reactivity.[56] However, there is no correlation between time and irradiation parameters for soft-start methods.[57]

3.2. Type and quantity of inorganic fillings – the increase in the amount of filler in photocurable dental resin

Since 1950, adding more inorganic[58] and/or nanogels[59,60] fillers has been the main method for minimizing polymerization shrinkage, which results in a decrease in the quantity of organic matrixes in the material. One of the most used fillers is silicon dioxide, which is available in crystal, colloidal, and pyrolytic forms,[61] as well as aluminum–lithium boron glass. When nanofiller is used, the amount of this component in composite materials—particularly those based on acrylic monomers—can even reach up to 90% of the mass.[62] Zinc oxide is also popular. For example, Pratap *et al.* added different amounts of micro sized zinc oxide (0%, 3%, 6% and 9%) to the standard monomer mixture used in the production of BisGMA/TEGDMA dental composites. They then showed that polymerization shrinkage was reduced from 15.2% for compositions without filler to 8.2% for compositions with 9% inorganic filler by weight.[136]

Moreover polyhedraloligomericsilsesquioxane (POSS) is a filler that is increasingly being used to improve the mechanical properties of such composites (POSS). The addition of POOS to the organic matrix can significantly reduce the risk of microleakage and secondary caries.[63] By adding this amount of filler to the volume of the composite, the stresses that would otherwise develop during the polymerization reaction are reduced, limiting the deleterious effects of shrinkage.

Nevertheless, by increasing the amount of the filler, the limit value when further shrinkage reduction became impossible has been obtained very quickly. Moreover, a significant amount of the filler, reaching even up to 70%, limits the depth of light penetration into the layer of the composite undergoing the process of photopolymerization, and then the entire conversion of the monomer does not occur.[64] Uneven and incomplete photopolymerization of acrylates and methacrylates leads to the leaching of unreacted monomers, where diffused from saliva filling, enters the gastrointestinal tract and further into the bloodstream. Unbound monomers can cause severe allergic and cytotoxic reactions.[65]

3.3. Type of organic matrix – application of alternative monomers

3.3.1. Use of silorane-based monomers. Sato *et al.* created organosilicon compounds containing oxirane for the first time in 1976.[66] Similar compounds were studied by Crivello *et al.*[67–69] in the early 1990s. These monomers produced effects that were both intriguing and feasible from a business standpoint. The name "siloxane" was created by 3M-ESPE to describe monomers that include both oxirane and siloxane units.[70] These monomers have found applications in the dental industry. They have hydrophobic properties due to their siloxane backbone, and low value polymerization shrinkage is brought on by the cycloaliphatic oxirane molecules that make up their structure. These monomers undergo local volumetric expansion to "open up" their molecular structures. This can thus compensate for polymerization shrinkage resulting from C=C or equivalent polymerization to some extent.[64] Comparing the siloxane-based composite system to methacrylates with average mechanical characteristics and high biocompatibility, the siloxane-based composite system exhibits better hydrophobicity and much lower polymerization stress and polymerization shrinkage. When siloxanes are used to create dental composites, polymerization shrinkage is guaranteed to be reduced by up to 0.94%.[71]

However, some studies demonstrated no beneficial effects of using siloxane-based monomers with regard to stress reduction,[72,73] In particular, siloxanes have been introduced

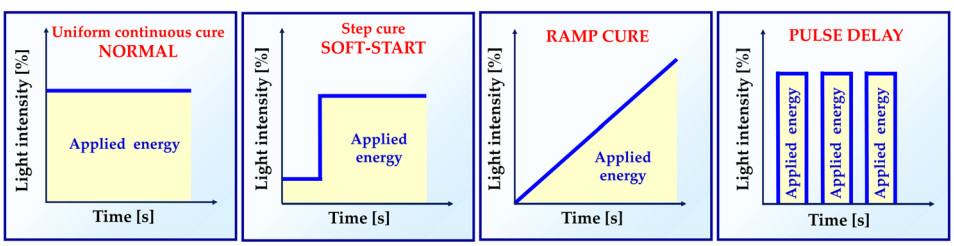

Fig. 5 Different dental light-curing modes.

into dentistry as promising alternatives for overcoming the negative effects of the shrinkage stress of polymerization. However, these compounds are currently not as attractive as was thought just a few years ago (Fig. 6).

3.3.2. Use of spiroothoesters (SOEs) or spiroorthocarbonates (SOCs). The next approach to reducing polymerization shrinkage is to use expanding monomers, which undergo volume expansion when polymerized. Spiroorthoesters (SOEs) and spiroorthocarbonates (SOCs) are the most widely studied expanding monomers (Fig. 7).

SOCs are double-cyclic acetals that polymerize when catalyzed in an acidic environment but remain stable in a basic environment. Double ring-opening photopolymerization (ROP) produces polymers from these chemicals (ethercarbonates). Due to the rise in excluded free volume brought on by the ring-opening procedure, ROP-cured bicyclic compounds often shrink less during the curing process. Bicyclic substances that can be employed as expansion co-monomers in resin-based composite formulations, such as spiro-orthocarbonates (SOCs), have been the subject of research by Bailey *et al.*[74] Expansion (3.5%) brought on by ring-opening interactions with SOCs can counterbalance the natural contraction. Nevertheless SOCs show poor solubility, minimal copolymerization, partial ring-opening, and negligible shrinkage reduction in dimethacrylate resins.

3.3.3. Use of tetraoxaspiroalkanes. Cecil C. Chappelow *et al.*[75] took a step further and synthesized and evaluated a new tetraoxaspiroalkane monomer containing silicon in siloxane-based systems. They explained that tetraoxaspiroalkanes polymerize *via* cationic mechanism, similarly to siloxanes. They then demonstrated that formulations containing tetraoxaspiroalkane monomers exhibited photopolymerization stress that were 40–99% less than the no addition control such as silorane-based resin (methylbis[2-(7-oxabicyclo[4.1.0]hept-3-yl) ethyl]phenylsilane and 2,4,6,8-tetramethyl-2,4,6,8-tetrakis-[2-(7-oxabicyclo[4.1.0]hept-3-yl)ethyl]-1,3,5,7-tetraoxa-2,4,6,8-tetrasilacyclooxetane). Examples of tetraoxaspiroalkane derivative structures are presented in Fig. 8.

3.3.4. Change the functional groups in monomers to vinylcyclopropanes (VCPs). Replacement of methacrylates (MAs) with cyclic monomers such as vinylcyclopropanes (VCPs) reduces shrinkage stress.[76] The decrease in shrinkage stress for VCP-containing compositions was first observed for 1,1-disubstituted 2-vinylcyclopropanes.[77] Both radical-stabilizing and electron-withdrawing groups boost the free-radical ring-opening propensity of very easily accessible 1,1-disubstituted 2-vinylcyclopropanes (Fig. 9).

The high-reactivity substitute structure for a commonly used urethane dimethacrylate (UDMA) that incorporates VCPs was developed by Contreras *et al.*[79] They demonstrated that, VCPs with urethane groups have extremely low shrinkage stress values. While being less reactive than methacrylates, crosslinking vinylcyclopropanes are utilized to promote the

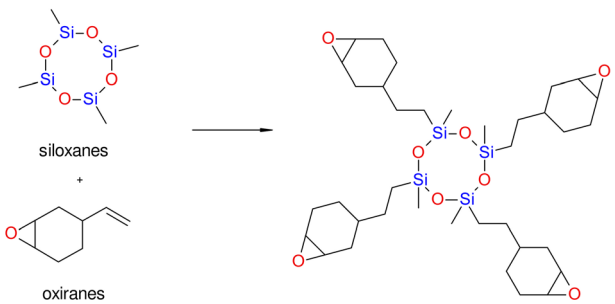

Fig. 6 Scheme of obtaining siloxane monomers.

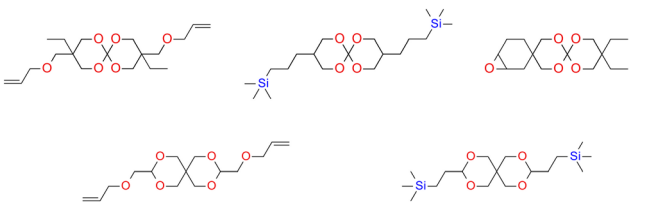

Fig. 8 Structures of oxaspirocyclic monomers.

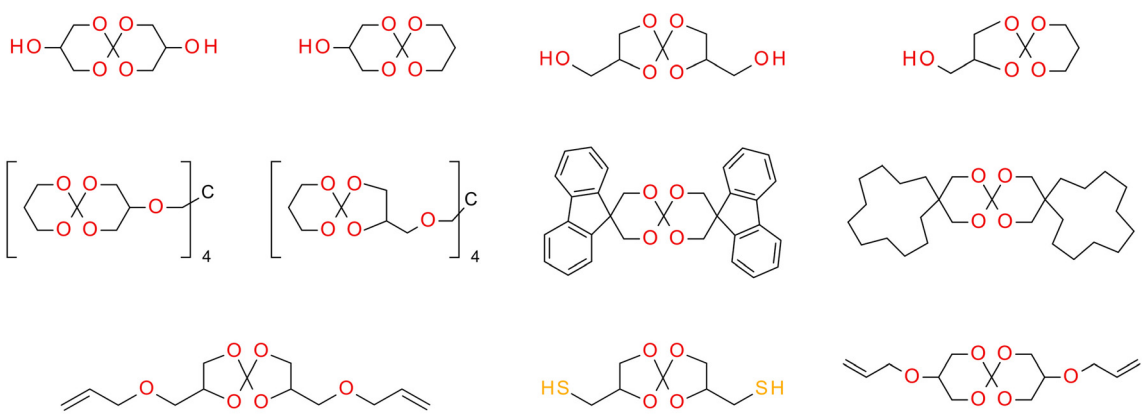

Fig. 7 Structures of spiroorthoesters (SOEs) and spiroorthocarbonates (SOCs).

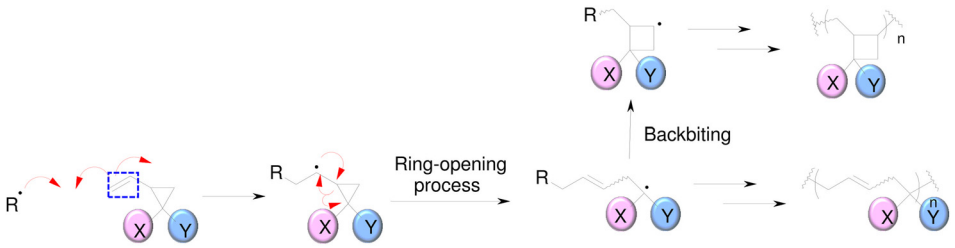

Fig. 9 Radical polymerization of 1,1-disubsituted 2-vinylcyclopropanes (VCPs).[78]

network formation of mixes of crosslinking vinylcyclopropanes and dimethacrylates.[80]

The structures of exemplary vinyl cyclopropanes are shown in Fig. 10.

3.3.5. Shifting the polymerization method of methacrylates from conventional free-radical chain-growth polymerization to affect network structure development (AFCT reagents). Thiol–ene[82] or thiol–yne[83,84] systems are another tried-and-true method for reducing shrinkage stress brought on by polymerization. Compared to formulations based on free-radical (meth)acrylate photopolymerization; the thiol–ene-based photocurable resins have several benefits. Thiols firstly relieve the oxygen inhibition by acting as strong hydrogen donors to a generated peroxide radical, which in turn produces a reactive thiyl radical.[85] Second, composites polymerize *via* thiol–ene mechanism exhibit lower shrinkage stress than acrylate resins. This is mostly due to the presence of gel point at relatively high conversion (>30%), which is caused by step-growth process of thiol–ene.[86] Finally, thiol–ene systems are more biocompatible than (meth)acrylate-based networks.[87] Thiol–ene polymerization is a great way to create polymers with specific network structures. While thiol–ene reactions are very efficient, they are restricted in terms of final formulation stability,[88] frequently display disagreeable odor,[89] and frequently suffer from softness and low T_g due to their thio-ether bridges.[90]

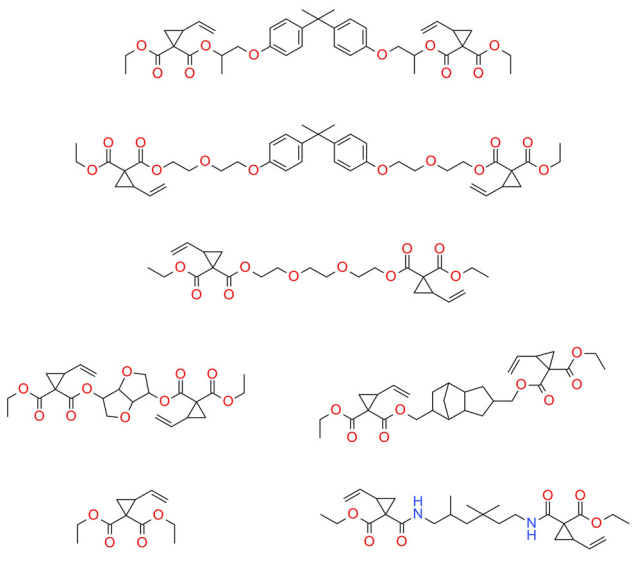

Fig. 10 Examples of vinyl cyclopropanes.[78,81]

Since it is known that (meth)acrylate-based photocurable systems result in brittle materials because of their uneven and heavily crosslinked network structure, work has been done to increase homogeneity and, consequently, the toughness of the photocurable dental compositions to comply with the demands of these materials. A (meth)acrylate[91] and thiol–ene systems[92] can be modified to contain addition–fragmentation chain transfer (AFCT) reagents to control the generation of radical networks (*via* chain transfer reaction). It is well known that multifunctional monomers (*i.e.*, diacrylates and triacrylates) undergo auto-acceleration in the initial phase of chain growth (free-radical) polymerization due to the fact that termination reactions are limited by mobility. A large kinetic chain length would result in the formation of a network with low homogeneity and high brittleness, which is less effective in stress dissipation, and therefore the shrinkage stress is a higher value.[93] Regulation of the final polymer architecture can be achieved using add–fragmentation chain transfer (*i.e.*, AFCT) agents.

The advantage of AFCT functional groups is that they facilitate stress relaxation during the polymerization process. During the process, the bonds are broken and the exact same chemical structure that existed prior to the bond breaking is reconstituted, leading to a rearrangement of the cross-linked strands.[92,94,95] For this reason, the approach concentrates on stress dissipation rather than volume shrinkage reduction. The allyl sulphide functional group of AFCT has been incorporated into both thiol–ene[53] and thiol-tin[96] reactions, yielding significant reductions in polymerization stress.

The reversibility of the AFCT mechanism is only possible for thiol-containing resins, as AFCT involving allyl sulphide requires the presence of thiyl radicals (Fig. 11). Nevertheless, it has also been proven that the introduction of allyl sulphide into methacrylate resins leads to a reduction in stress, but this effect decreases with increasing methacrylate content.[97] The presence of a carbon-centred radical in the photopolymerization of methacrylate results to an irreversible AFCT of the allyl sulphide group (Fig. 12).

This AFCT reagent reduces the crosslinking density, favoring a more linear growth of the polymer chain, which shifts the gel point towards higher conversion values and finally reduces the shrinkage stress of the polymerization.[98] Therefore, the use of AFCT results in the formation of homo-

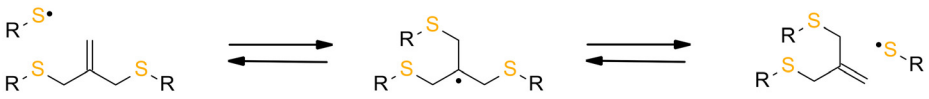

Fig. 11 Schematic of the mechanism of allyl sulfide AFCT in the presence of a thiyl radical. The reaction leads to the formation of a reversible symmetric chemical structure.

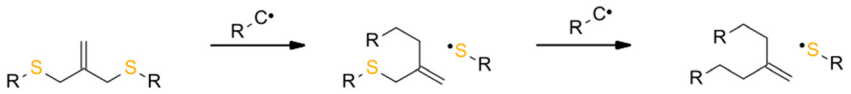

Fig. 12 Schematic of the mechanism of allyl sulphide AFCT in the presence of a carbon centre radical. The reaction leads to an asymmetric chemical structure, the reaction is irreversible.

geneous networks and hence provides high toughness networks.[99] The implementation of chain transfer *via* the AFCT mechanism can reduce the shrinkage stress observed in free-radical photopolymerization systems.

The mechanism of addition–fragmentation chain transfer for an ethyl ester activated vinyl sulfone ester (EVS) is presented in Fig. 13.

Hamad Algamaiah *et al.* confirmed that Tetric PowerFill composite (PFill) contains an addition fragmentation chain transfer (AFCT) agent characterized by reduced polymerization shrinkage.[100]

3.3.6. Shifting the polymerization method of methacrylates from conventional free-radical chain-growth polymerization to affect network structure development (RAFT reagents). The trithiocarbonate functional group is often utilized as a reversible addition–fragmentation chain transfer (RAFT) agent for the synthesis of polymers with low polydispersity.[101] In contrast to the allyl sulphide functional group, the trithiocarbonate functional group is able to completely reversible AFCT when it reacts with a carbon-centred radical, such as that present in the polymerisation of methacrylate (Fig. 14). Park *et al.* investigated bisphenylglycidyl dimethacrylate/triethylene glycol dimethacrylate BisGMA-TEGDMA-based and BisGMA-TTCDMA (S,S′-bis[α,α′-dimethyl-α″-(acetyloxy)ethyl 2-methyl-2-propenoate]-trithiocarbonate) containing triocarbonate dental composites to demonstrate stress relaxation *via* RAFT. The trithiocarbonate functional group was introduced to effectively induce RAFT, leading to network rearrangement. The researchers showed that the incorporation of this mechanism resulted in a 65% stress reduction compared to the standard BisGMA-TEGDMA composite.[102]

3.4. Type of photoinitiators

Type of photoinitiator in resins for dental applications have influence on degree of conversion and reaction kinetics which was described in the previous article.[39] Furthermore, the type and amount of photoinitiators also affects the value of polymerization shrinkage of dental compositions. To date, the most common resin photoinitiator system in the dental industry has been camphoroquinone (CQ) and co initiators in the form of amine derivatives.[103–106] For example, it has been demonstrated that reducing the CQ-amine content to approximately half, results in a reduction in conversion rate, polymerization rate and polymerization shrinkage from 17.6% to 5.5%.[107] In other studies, it was reported, commercially available dental fillings with additional photoinitiators such as Lucirin TPO and Ivocerin have the lowest polymerisation shrinkage (*e.g.* Tetric EvoCeram Bleach BLXL containing Camphorquinone, Lucirin TPO or Tetric Evoceram Powerfill IVB containing Camphorquinone, tertiary amines, Ivocerin,

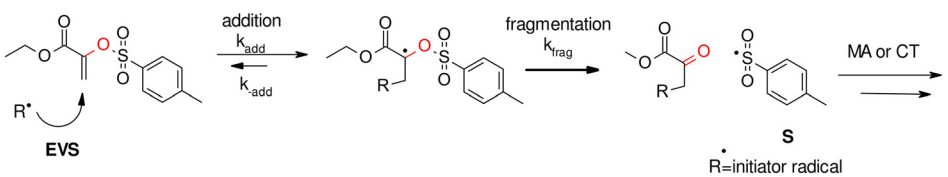

Fig. 13 AFCT mechanism for an ethyl ester activated vinyl sulfone ester (EVS).

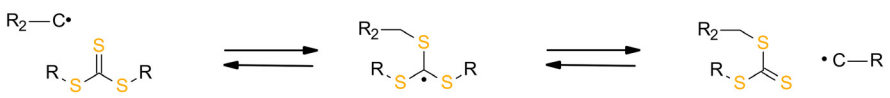

Fig. 14 Schematic of the RAFT mechanism of a trithiocarbonate in the presence of a carbon centered radical. The reaction leads to a symmetric chemical structure, the reaction is reversible.

TPO) than dental fillings containing only CQ and tertiary amines (Filtek Ultimate A2).[108] Indeed, experimental resins containing 1-phenyl-1,2-propanedione/PPD[109] and monoacylphosphine/MAPO[109] were proved to induce lower stresses compared to a control system containing only CQ. In contrast, PPD was found to slow down the resin polymerization reaction, allowing greater stress relaxation; whereas MAPO showed a more complex stress reduction mechanism. This mechanism was involved in both delaying the diffusion-controlled polymerization propagation step and increasing the reaction temperature, allowing greater reaction mobility, greater stress relaxation and a delayed onset of vitrification compared to the CQ-based resin.

The summary of the polymerization shrinkage values and their respective reduction for different composition variants is shown in Table 2.

Table 2 Table to present the shrinkage values and relevant reduction of different compositions

Composition/factor leading to lower polymerization shrinkage	Polymerization shrinkage value	Ref.
Standard acrylate monomers	Polymerization shrinkage of acrylate monomers oscillates at 2–14%	45
Replacement of TEGDMA monomer with allyl carbonate monomer (BPhADAC)	The reduction in shrinkage from 5.37% to 4.48%.	135
Addition of 9% w/w zinc oxide to standard BisGMA/TEGDMA organic matrix	The reduction in shrinkage from 15.2% to 8.2%	136
Reducing CQ-amine content to approximately half	The reduction in shrinkage from 17.6% to 5.5%	107
Silorane monomer	0.94%	71

4. Conventional and new methods for measuring polymerization shrinkage of dental composites

The numerous of methods for the determination of polymerization shrinkage of dental composite restorative materials have been described in the literature (Table 3). This section presents the main methods of determining the polymerization shrinkage.

Table 3 Summary of methods for measuring polymerization shrinkage

Methods	Advantage	Disadvantage
Dilatometry[128]	• Fast • Simple	• Temperature sensitivity of the mercury in the column • Potential health hazards
Linometery	• Fast • Simple • Insensitive to temperature changes producing constant results	• The technique is based on measuring linear shrinkage using contact displacement transducers. • There may be potential errors due to gravity or non-uniform shrinkage of the sample
Gas pschychometry[128]	• Not time-consuming • Temperature-independent method • Helium can occupy voids in a material because helium molecules are much smaller than water.	• Method showing only the final shrinkage
Strain gauge[110]	• Very sensitive to linear dimensional changes	• Difficulty in placing and holding bulk material samples of sufficient thickness on the strain gauge.
Archimedes principle (buoyancy method)[124]	• It is the only method for measuring polymerization shrinkage that has published performance standards in ISO 17304	• Multi-step, time-consuming and requires the consideration of a number of variables *e.g.* the presence of voids inside the specimen or air bubbles on the surface of the specimen
The bonded-disk method[110]	• Simple design • Does not require expensive instrumentation • The thickness of the samples is small and, therefore, light easily penetrates the material. This ensures equal conversion of the monomer on the top and bottom surfaces and consequently over the entire thickness	• Can only be used for relatively thin samples
Optical coherence tomography (OCT)	• Non-invasive and non-contact medical diagnostic imaging modality • Produces both high-resolution images of teeth and periodontal tissues without exposing the patient to ionising radiation	• Expensive
X-ray microcomputed tomography	• High-resolution X-ray μCT allows 3D information	• Expensive apparatus
AcuVol™	• Easy-to-use device for tracking polymerization shrinkage throughout the curing process • Accurate measurements of polymerization shrinkage	• Expensive apparatus
Digital image correlation (DIC)	• Full-field sample measurement • Providing more detailed and useful information on the shrinkage	• Expensive apparatus

4.1. Dilatometry

Dilatometry is the most widely applied method for determining polymerization shrinkage. In this method, a non-reactive liquid, such as mercury, surrounds the composite sample during curing. Monitoring the level of mercury in the capillary allows the operator to measure the volume shrinkage (VS) associated with the polymerization of the sample. Thus, the amount of shrinkage is recorded, given that the shrinkage is monitored during the curing period from pre-gel to post-gel phase.[110] The disadvantage of the dilatometers is that they are extremely sensitive to variations in temperature.[111,112]

A recording dilatometer for measuring polymerization shrinkage was described as early as the second half of the 20th century and is still employed today.[113,114] For instance, Wang *et al.* in 2018 measured the polymerization shrinkage of dental resin composites with hydrolytically stable monomers consisting of UDMA and hydrolytically stable triethylene glycol-divinylbenzyl ether TEG-DVBE using a mercury dilatometer (ADA Foundation, Gaithersburg, MD, USA).[113] The measurement consisted of placing approximately 0.1 g of the composite on a sandblasted and silanised glass slide. The glass column was clamped onto the slide and filled with mercury. After this, an LVDT (linear variable differential transducer) probe was placed on the slide. The composite was light-cured through the glass slide.[115] The modified mercury dilatometer has also been proposed, in which each change in sample volume is recorded every 0.5 s as a change in the height of the mercury in the capillary, which is measured electronically instead of with the naked eye. The device is relatively inexpensive and allows measurements to be made on samples regardless of shape and size.[111]

4.2. Linometery

In 1969, Lee *et al.* from California determined linear polymerization shrinkage using a dilatometer to the nearest 0.00005 inch on a cylinder. The measurement consisted of placing a portion of the mixture into a glass tube 6.35 mm in diameter and approximately 9.5 mm long. The plunger was then pressed into the mixed material and the dilatometer was zeroed within 45 seconds of mixing. The sample was left to cure at room temperature for 18 h. The percentage of shrinkage was calculated from:

$$\text{Shrinkage} = \frac{\Delta L}{L + \Delta L} \times 100\%$$

where: ΔL – change in length, L – cured length.

The average of five readings was taken for each material.[116]

A few years later, 1993, de Gee *et al.* introduced a modified linometer that was quite simple, fast and insensitive to temperature changes, giving constant results. They found no significant differences between this method and dilatometry. A composite sample was placed between a glass and an aluminum disc. The distance from the aluminum disc to the glass could be adjusted using a displacement transducer to select the height of the resin sample. The disc and glass were lubricated to avoid adhesion of the composite sample. However, this apparatus only measured linear changes.[117] It is worth noting that there are no significant differences between this method and dilatometry.

Interestingly, the method was described by Shah *et al.* in 2010 for measuring linear shrinkage measurements using a rheometer.[118] Nejadebrahim in 2019 determined polymerization shrinkage with a new three-component safranin-based photoinitiating system using an Anton Paar MCR 302 rheometer, which was combined with accessories for light-curing samples. The test was carried out in the oscillatory mode of the rheometer. The smooth aluminum plate was fixated at an initial gap of 0.5 mm and a zero Newton normal force was applied to the samples. An optical fibre was placed perpendicularly under the glass plate to allow the curing process to take place. With polymerization shrinkage, the gap was decreased. The polymerization shrinkage was calculated from the formula:[119]

$$\%\text{Shrinkage} = \left(1 - \frac{d_{\text{final}}}{d_{\text{initial}}}\right) \times 100$$

where: d_{final} – distances between the glass and aluminum plate at the beginning of photopolymerization, d_{initial} – distances between the glass and aluminum plate at the beginning of photopolymerization.

The experimental setup is presented in Fig. 15.

Polymerization shrinkage is also common in photo-cured 3D printing, due to the fact that the base material is also acrylate monomers are characterized by high polymerization

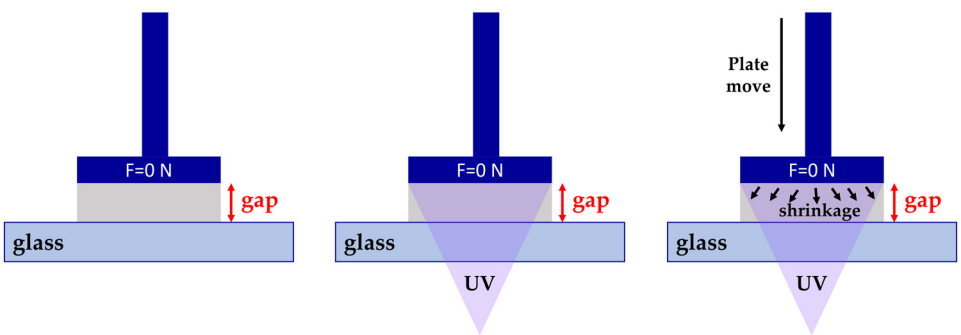

Fig. 15 Schematic representation of the shrinkage measurement apparatus.

shrinkage. Therefore, polymerization shrinkage tests using a rheometer are becoming increasingly popular and are also used to measure the polymerization shrinkage of objects used in 3D printing.[120]

4.3. Gas pschychometry

In 1999, Cook *et al.* used a non-contact method called a displacement pycnometer to determine the dry volume changes of composite materials during the polymerization process. The disadvantage of this method is that it only measures the final shrinkage. Nevertheless, the advantage of this method is that it is not time-consuming.

The standard measurement is that a sample of the composite paste is placed between two small sheets of thin Mylar sheet. The volume of the sample including the Mylar sheets is then determined at constant room temperature (23 °C ± 2 °C) using a controlled helium tank gas pycnometer.

The volume of the sample placed in the chamber is determined by varying the helium pressure. Then, after curing, the volume of the composite sample and Mylar sheets is determined again, and the difference between the uncured and cured samples (ΔV) is calculated. The Mylar sheets are then removed from the sample and the volume (V) of the cured sample itself is determined. The quantification of the percentage shrinkage (S) is determined using the formula:[121]

$$\text{Shrinkage}(S) = \left(\frac{\Delta V}{V + \Delta V}\right) \times 100$$

ΔV – difference between the uncured and cured samples, V – volume of the cured sample.

4.4. Strain gauge

Strain gauge are very sensitive to linear dimensional changes. Here, the gauge is connected to the substrate and the linear dimensional changes occurring in the substrate are transferred to the gauge and measured. This method can be applied to measure the post-gel shrinkage of composites. This is because the substrate has a measurable modulus, to induce stress on the gauge, the linear dimensional changes will be transferred to the gauge.[122]

4.5. Archimedes principle

Archimedes' principle (buoyancy of a material in a liquid) is a simple and inexpensive method that has been used to determine the volume change of a sample by measuring density changes.[123] The method involves weighing materials several times in two environments of known density: one is conventional air, the other can be distilled water, siliconized oil, mercury and sodium lauryl sulphate of at least 99% purity.[124]

$$\rho = \frac{m_{\text{water}}}{m_{\text{air}} - m_{\text{water}}}(\rho_{\text{water}} - \rho_{\text{air}}) + \rho_{\text{air}}$$

ρ – density of the materials, m_{water} – mass of sample in water (g), m_{air} – mass of sample in air (g), ρ_{water} – density of water at a precisely measured temperature, ρ_{air} – density of the air (air density: 0.0012 g cm^{-1}).[124]

In turn, the change in volume is calculated:

$$\Delta V = \left(\frac{1}{\rho_{15\ \text{min}}} - \frac{1}{\rho_{\text{uncure}}}\right)\frac{1}{\rho_{\text{uncure}}} \times 100\%$$

In this method, sample size and geometry are not considered a problem when applying Archimedes' principles. The process is multi-step, time-consuming and requires the consideration of a number of variables *e.g.* the presence of voids inside the specimen or air bubbles on the surface of the specimen, which may affect the test results. Nevertheless, it is the only method for measuring polymerization shrinkage that has published performance standards in ISO 17304.[124] Therefore, this method is popular for determining the polymerization shrinkage of dental composites.[44,125,126] For example, Zhao *et al.* studied the polymerization shrinkage by this method of hybrid composites used for 3D printing of tooth crowns.[127]

4.6. The bonded-disk method

The method was developed in 1991 by Watts and Cash.[128] The method involves placing a disc of resin composite in a brass ring (16 mm × 1.5 mm), which is bonded to a glass slide. The composite is covered with a microscope coverslip (approximately 0.1 mm thick). The composite sample is cured from below by the glass slide. As the composite shrinks, it pulls the coverslip downwards and its deflection is monitored by the linear vertical displacement transducer (LVDT) probe attached to the middle of the coverslip. Shrinkage is calculated by dividing the measured deflection of the coverslip by the initial height of the composite. Because the composite sample must exhibit some stiffness to flex the slide, this method is likely to measure shrinkage after gelling.[128]

4.7. Optical coherence tomography (OCT)

OCT is a non-invasive and non-contact medical diagnostic imaging modality. The principle of OCT is analogous to methods such as CT, MRI and B-scan ultrasonography, which use X-rays, spin resonance and sound waves respectively, except that only light is used.

OCT is based on a Michelson interferometer with a low-coherence and broadband light source. The apparatus consists of a scanning probe, a base unit containing a superluminescent diode as light source and a computer. In this method, 3 scans are performed: first, a scan is performed on a hollow cylindrical mould made of Teflon, then the composite is introduced and a 2nd scan is performed, followed by a 3rd scan after 15 minutes of photo-curing. The linear shrinkage is calculated from the formula:

$$\text{Shrinkage}[\%] = \left(\frac{\text{RC}_{0\ \text{min}} - \text{RC}_{15\ \text{min}}}{\text{RC}_{0\ \text{min}}}\right) \times 100\%$$

$\text{RC}_{0\ \text{min}}$ – thickness of the composition between 1 and 3 points of unpolymerized state, $\text{RC}_{15\ \text{min}}$ – thickness of the composition between 1 and 3 of the polymerized state.

The OCT technique produces both high-resolution images of teeth and periodontal tissues without exposing the patient to ionising radiation.[44]

4.8. X-ray microcomputed tomography (μCT)

X-ray microcomputed tomography (μCT) is used to study the 3D marginal adaptation of light-cured composite resin restorations and the tooth-composite interface. In addition, high-resolution X-ray μCT allows 3D information to be obtained from the cavity during the polymerization process. This method for determining polymerization shrinkage was used by Rizzante *et al.* In the same work, he showed a strong correlation between filler content and volumetric shrinkage, the higher the inorganic filler content, the lower the polymerization shrinkage.[129] Sampaio *et al.* have shown that both μCT and OCT techniques can be used to detect pulp floor fissures in restorations.[48]

4.9. AcuVol™

The AcuVol instrument from Biso applies the video imaging method and allows accurate measurements of polymerization shrinkage. This device includes a table-top instrument that can be connected to a computer. This method enables comparison of the volume of composites before curing (before polymerization shrinkage) and after curing (after polymerization shrinkage). In addition, it is an easy-to-use device for tracking polymerization shrinkage throughout the curing process.[130]

Dano *et al.* investigated the polymerization shrinkage of oxirane/acrylate interpenetrating polymer network (IPN) composite resins using the AcuVol™ video imaging technique. Low volumes of samples (~15 μl) of the composite material were placed in the AcuVol and cured from above. During the measurement, images are generated that simultaneously show the sample before and after curing. It registers the relative change in volume (shrinkage). In addition, a titanium dioxide pigment (0.01 wt%) was introduced into the monomers to ensure accurate identification of the droplet outline by the imaging software.[131] Ender Akan studied the effect of the shade of adhesive resin cement on its polymerization shrinkage using the AcuVol technique. He demonstrated that different shades showed different volumetric shrinkage. Group 5 (opaque yellow, 2.62%) and group 2 (universal, brown, 3.96%) showed the lowest and highest percentage of shrinkage, respectively.[127] Using this device, Canellas *et al*. determined the polymerization shrinkage of dental composites containing methacrylethylpolyhedral oligomeric silsesquioxane (ME-POSS) and showed that the addition of this compound reduces the polymerization shrinkage of composites.[134]

4.10. Digital image correlation (DIC)

Digital image correlation is a non-contact method that was developed in the 1980s at the University of South Carolina. The idea of the method is to visualize patterns on the surface of the sample from sequential images taken during the deformation of the material in a full-field measurement, which allows displacement and deformation to be determined by tracing movements on the surface of the sample. The full-field measurement capability enables accurate analysis of inhomogeneous deformations and stresses.[130,132] This allows more accurate decisions to be made regarding the choice of appropriate materials and embedding techniques for the restoration of damaged or decayed teeth.

4.11. Future insights

Major progress has been achieved in reducing polymerization shrinkage in dental composites. However, considering the complexity of the problem due to the dependence of polymerization shrinkage on numerous factors such as the type of monomer, initiators, curing methods and curing time, the researchers are still looking for a dental material characterized not only by a low polymerization shrinkage of less than 1%, but also a lack of toxicity, complete reactivity of the monomer to the polymer, good mechanical properties and a cheap. Therefore, the issue of producing dental composites with low polymerization shrinkage is still a topic that is being addressed by researchers from different areas of the world.

5. Conclusion

This paper presents the influence of the choice of photopolymerization process conditions and also the composition of the composition on the polymerization shrinkage of dental composites. In particular, it was demonstrated that the polymerization shrinkage of dental composites depends on the type of monomers, photoinitiators, the type and amount of inorganic fillers and the curing method. This paper presents alterative curing mechanisms, alternative monomers, photoinitiators, and inorganic fillers and curing method to minimize undesirable polymerization shrinkage in dental composites. The second section demonstrates standard and novel methods for testing the polymerization shrinkage. It is shown that each method has its own advantages and disadvantages. In addition, due to the diversity of apparatus performance, polymerization shrinkage values should be assessed using the same analytical method. It is also necessary to have a standardized apparatus to compare polymerization shrinkage for different dental fillings. In addition, researchers are still looking for a dental material characterized by low polymerization shrinkage but also a lack of toxicity, complete reactivity of the monomer to the polymer, good mechanical properties and a low cost.

Conflicts of interest

The authors declare no conflict of interest.

Note added after first publication

This article replaces the version published on 28 April 2023 which was missing funding information in the Acknowledgements section.

Acknowledgements

The work was funded by the National Science Centre (NCN, Poland), PRELUDIUM 17, project no: 2019/33/N/ST5/03015. One of the authors M.T.S. would like to thank Foundation for Polish Science (Warsaw, Poland), project START, Grant No. START 088.2023.

References

1 J. V. Crivello, *J. Macromol. Sci., Part A: Pure Appl. Chem.*, 2015, **52**, 336–344.
2 V. A. Bobrin, Y. Yao, X. Shi, Y. Xiu, J. Zhang, N. Corrigan and C. Boyer, *Nat. Commun.*, 2022, **13**, 3577.
3 J. Ortyl, M. Galica, R. Popielarz and D. Bogdał, *Pol. J. Chem. Technol.*, 2014, **16**, 75–80.
4 E. Hola, M. Topa, A. Chachaj-Brekiesz, M. Pilch, P. Fiedor, M. Galek and J. Ortyl, *RSC Adv.*, 2020, **10**, 7509–7522.
5 M. Topa, E. Hola, M. Galek, F. Petko, M. Pilch, R. Popielarz, F. B. G. Morlet-Savary, J. Laleveé and J. Ortyl, *Polym. Chem.*, 2020, **11**, 5261–5278.
6 Z. Liu and F. Dumur, *Eur. Polym. J.*, 2022, **177**, 111449.
7 A. Al Mousawi, C. Dietlin, B. Graff, F. Morlet-Savary, J. Toufaily, T. Hamieh, J. P. Fouassier, A. Chachaj-Brekiesz, J. Ortyl and J. Lalevée, *Macromol. Chem. Phys.*, 2016, **217**, 1955–1965.
8 M. Topa, F. Petko, M. Galek, M. Jankowska, R. Popielarz and J. Ortyl, *Eur. Polym. J.*, 2021, **156**, 110612.
9 H. C. Kiliclar, G. Yilmaz, Z. Li, Y. Zheng and Y. Yagci, *Macromol. Chem. Phys.*, 2023, **224**, 2200343.
10 M. Topa, F. Petko, M. Galek and J. Ortyl, *Sensors*, 2020, **20**, 3043.
11 J. Shao, Y. Huang and Q. Fan, *Polym. Chem.*, 2014, **5**, 4195–4210.
12 W. Tomal, M. Pilch, A. Chachaj-Brekiesz, M. Galek, F. Morlet-Savary, B. Graff, C. Dietlin, J. Lalevée and J. Ortyl, *Polym. Chem.*, 2020, **11**, 4604–4621.
13 E. Hola, M. Pilch, M. Galek and J. Ortyl, *Polym. Chem.*, 2020, **11**, 480–495.
14 M. Bouzrati-Zerelli, J. Kirschner, C. P. Fik, M. Maier, C. Dietlin, F. Morlet-Savary, J. P. Fouassier, J. M. Becht, J. E. Klee and J. Lalevée, *Macromolecules*, 2017, **50**, 6911–6923.
15 J. Ortyl, K. Sawicz and R. Popielarz, *J. Polym. Sci., Part A: Polym. Chem.*, 2010, **48**, 4522–4528.
16 J. Ortyl, J. Wilamowski, P. Milart, M. Galek and R. Popielarz, *Polym. Test.*, 2015, **48**, 151–159.
17 J. Ortyl, M. Galek, P. Milart and R. Popielarz, *Polym. Test.*, 2012, **31**, 466–473.
18 N. Moszner, *Macromol. Symp.*, 2004, **217**, 63–76.
19 K. Yoshinaga, K. Yoshihara and Y. Yoshida, *Dent. Mater.*, 2021, **37**, e391–e398.
20 A. Bagheri and J. Jin, *ACS Appl. Polym. Mater.*, 2019, **1**, 593–611.
21 A. Jandyal, I. Chaturvedi, I. Wazir, A. Raina, M. Irfan and U. Haq, *Sustainable Oper. Comput.*, 2022, **3**, 33–42.
22 A. Kowalska, J. Sokolowski and K. Bociong, *Polymers*, 2021, **13**, 1–17.
23 M. Topa and J. Ortyl, *J. Photopolym. Sci. Technol.*, 2021, **34**, 259–262.
24 M. V. Salvador, B. M. Fronza, V. G. A. Pecorari, F. A. Ogliari, R. R. Braga, J. D. Oxman and A. F. Lima, *Dent. Mater.*, 2021, **37**, 1358–1365.
25 A. A. Pérez-Mondragón, C. E. Cuevas-Suárez, J. A. González-López, N. Trejo-Carbajal and A. M. Herrera-González, *J. Photochem. Photobiol., A*, 2020, **403**, 112844.
26 M. Topa and J. Ortyl, *Materials*, 2020, **13**, 4093.
27 J. He, S. Garoushi, E. Säilynoja, P. K. Vallittu and L. Lassila, *Dent. Mater.*, 2019, **35**, 627–635.
28 Y. R. Riva and S. F. Rahman, *AIP Conf. Proc.*, 2019, **2193**, 020011.
29 J. A. González-López, A. A. Pérez-Mondragón, C. E. Cuevas-Suárez, S. C. Esparza González and A. M. Herrera-González, *J. Mech. Behav. Biomed. Mater.*, 2020, **110**, 103955.
30 M. L. Berlanga Duarte, L. A. Reyna Medina, P. Torres Reyes, S. C. Esparza González and A. M. Herrera González, *J. Appl. Polym. Sci.*, 2019, **136**, 1–10.
31 Y. Catel, J. Angermann, P. Fässler, U. Fischer, T. Schnur and N. Moszner, *Dent. Mater.*, 2021, **37**, 351–358.
32 J. Wu, X. Xie, H. Zhou, F. R. Tay, M. D. Weir, M. A. S. Melo, T. W. Oates, N. Zhang, Q. Zhang and H. H. K. Xu, *Polym. Degrad. Stab.*, 2019, **163**, 87–99.
33 L. Song, Q. Ye, X. Ge, A. Misra, C. Tamerler and P. Spencer, *Acta Biomater.*, 2019, **83**, 130–139.
34 S. Venz and B. Dickens, *J. Biomed. Mater. Res.*, 1991, **25**, 1231–1248.
35 Y. Kinomoto, M. Torii, F. Takeshige and S. Ebisu, *J. Dent.*, 1999, **27**, 383–389.
36 J. W. Park and J. L. Ferracane, *Dent. Mater.*, 2005, **21**, 882–889.
37 J. W. Park and J. L. Ferracane, *J. Dent. Res.*, 2006, **85**, 945–949.
38 A. J. Feilzer, A. J. de Gee and C. L. Davidson, *J. Dent. Res.*, 1987, **66**, 1636–1639.
39 R. R. Braga, R. Y. Ballester and J. L. Ferracane, *Dent. Mater.*, 2005, **21**, 962–970.
40 T. Dikova, J. Maximov, V. Todorov, G. Georgiev and V. Panov, *Processes*, 2021, **9**, 779.
41 J. W. Stansbury, *J. Esthetic Restor. Dent.*, 2000, **12**, 300–308.
42 M. Daronch, F. A. Rueggeberg, M. F. De Goes and R. Giudici, *J. Dent. Res.*, 2006, **85**, 38–43.
43 A. Versluis, W. H. Douglas, M. Cross and R. L. Sakaguchi, *J. Dent. Res.*, 1996, **75**, 871–878.
44 P. Ausiello, A. M. d. O. Dal Piva, A. L. S. Borges, A. Lanzotti, F. Zamparini, E. Epifania and J. P. M. Tribst, *Appl. Sci.*, 2021, **11**, 1–12.
45 R. B. Price, A. S. Rizkalla and G. C. Hall, *Am. J. Dent.*, 2000, **13**, 176–180.

46 N. Ivković, D. Božović, S. Ristić, V. Mirjanić and O. Janković, *Contemp. Mater.*, 2013, **4**, 84–91.
47 K. Aalto-Korte, K. Alanko, O. Kuuliala and R. Jolanki, *Contact Dermatitis*, 2007, **57**, 324–330.
48 C. S. Sampaio, J. Fernández Arias, P. J. Atria, E. Cáceres, C. Pardo Díaz, A. Z. Freitas and R. Hirata, *Dent. Mater.*, 2019, **35**, 1568–1575.
49 J. L. Ferracane, *Oper. Dent.*, 2008, **33**, 247–257.
50 J. L. Ferracane, *Dent. Mater.*, 2005, **21**, 36–42.
51 R. Labella, P. Lambrechts, B. Van Meerbeek and G. Vanherle, *Dent. Mater.*, 1999, **15**, 128–137.
52 C. J. Kleverlaan and A. J. Feilzer, *Dent. Mater.*, 2005, **21**, 1150–1157.
53 Z. Tarle, T. Attin, D. Marovic, L. Andermatt, M. Ristic and T. T. Tauböck, *Clin. Oral Invest.*, 2015, **19**, 831–840.
54 H. Al Sunbul, N. Silikas and D. C. Watts, *Dent. Mater.*, 2016, **32**, 998–1006.
55 I. Aljosa, L. Tijana, B. Larisa and V. Marko, *Procedia Eng.*, 2014, **69**, 921–930.
56 R. C. B. Alonso, W. C. Brandt, E. J. C. Souza-Junior, R. M. Puppin-Rontani and M. A. C. Sinhoreti, *Appl. Adhes. Sci.*, 2014, **2**, 1–11.
57 C. A. K. Shimokawa, P. M. A. Carneiro, T. R. da S. Lobo, V. E. Arana-Chavez, M. N. Youssef and M. L. Turbino, *Int. Dent. J.*, 2016, **66**, 257–263.
58 Z. Wang, F. A. Landis, A. A. M. Giuseppetti, S. Lin-Gibson and M. Y. M. Chiang, *Dent. Mater.*, 2014, **30**, 1316–1324.
59 J. Han, S. Jiang, Y. Gao and F. Sun, *J. Mater. Chem. C*, 2016, **4**, 10675–10683.
60 R. R. Moraes, J. W. Garcia, M. D. Barros, S. H. Lewis, C. S. Pfeifer, J. Liu and J. W. Stansbury, *Dent. Mater.*, 2011, **27**, 509–519.
61 V. Greig, *Br. Dent. J.*, 2012, **213**, 90–90.
62 M. H. Chen, *J. Dent. Res.*, 2010, **89**, 549–560.
63 S. B. Burujeny, H. Yeganeh, M. Atai, H. Gholami and M. Sorayya, *Dent. Mater.*, 2017, **33**, 119–131.
64 Z. Wang and M. Y. M. Chiang, *Dent. Mater.*, 2016, **32**, 551–560.
65 K. S. Gregson, J. Terrence O'Neill, J. A. Platt and L. Jack Windsor, *Dent. Mater.*, 2008, **24**, 1461–1467.
66 Sato *et al.*, *JP Pat.*, 51033541, 1976.
67 J. V. Crivello, *Polym. Eng. Sci.*, 1992, **32**, 1462–1465.
68 J. V. Crivello and J. L. Lee, *J. Polym. Sci., Part A: Polym. Chem.*, 1990, **28**, 479–503.
69 P. H. Chung, J. V. Crivello and M. Fan, *J. Polym. Sci., Part A: Polym. Chem.*, 1993, **31**, 1741–1746.
70 J. D. Eick, S. P. Kotha, C. C. Chappelow, K. V. Kilway, G. J. Giese, A. G. Glaros and C. S. Pinzino, *Dent. Mater.*, 2007, **23**, 1011–1017.
71 N. Hamano, Y. C. Chiang, I. Nyamaa, H. Yamaguchi, S. Ino, R. Hickel and K. H. Kunzelmann, *Dent. Mater.*, 2012, **28**, 894–902.
72 G. Marchesi, L. Breschi, F. Antoniolli, R. Di Lenarda, J. Ferracane and M. Cadenaro, *Dent. Mater.*, 2010, **26**, 947–953.
73 A. R. Aleixo, R. D. Guiraldo, A. P. P. Fugolin, S. B. Berger, R. L. X. Consani, A. B. Correr, A. Gonini-Júnior and M. B. Lopes, *Photomed. Laser Surg.*, 2014, **32**, 267–273.
74 (*a*) W. J . Bailey and T. Endo, *J. polym. sci., Polym. symp.*, 2007, **64**, 17–26; (*b*) W. J. Bailey and R. L. Sun, *Polym. Prepr. (Am. Chem. Soc., Div. Polym. Chem.)*, 1972, **13**, 281; (*c*) T. Endo and W. J. Bailey, *J. Polym. Sci. Polym. Lett. Ed.*, 1980, **18**, 25.
75 C. Chappelow, C. Pinzino, S-S. Chen and J. D. Eick, US20070072954A1, 2006.
76 N. Moszner and U. Salz, *Macromol. Mater. Eng.*, 2007, **292**, 245–271.
77 F. Sanda, T. Takata and T. Endo, *Macromolecules*, 1993, **26**, 1818–1824.
78 S. Tauscher, Y. Catel, P. Fässler, U. Fischer and N. Moszner, *J. Appl. Polym. Sci.*, 2017, **134**, 1–9.
79 P. Pineda Contreras, C. Kuttner, A. Fery, U. Stahlschmidt, V. Jérôme, R. Freitag and S. Agarwal, *Chem. Commun.*, 2015, **51**, 11899–11902.
80 N. Moszner, T. Völkel, U. K. Fischer and V. Rheinberger, *Macromol. Rapid Commun.*, 1999, **20**, 33–35.
81 S. Schoerpf, Y. Catel, N. Moszner, C. Gorsche and R. Liska, *Polym. Chem.*, 2019, **10**, 1357–1366.
82 C. E. Hoyle and C. N. Bowman, *Angew. Chem., Int. Ed.*, 2010, **49**, 1540–1573.
83 R. Hoogenboom, *Angew. Chem., Int. Ed.*, 2010, **49**, 3415–3417.
84 A. Oesterreicher, C. Gorsche, S. Ayalur-Karunakaran, A. Moser, M. Edler, G. Pinter, S. Schlögl, R. Liska and T. Griesser, *Macromol. Rapid Commun.*, 2016, **37**, 1701–1706.
85 B. Husár, S. C. Ligon, H. Wutzel, H. Hoffmann and R. Liska, *Prog. Org. Coat.*, 2014, **77**, 1789–1798.
86 O. D. McNair, A. P. Janisse, D. E. Krzeminski, D. E. Brent, T. E. Gould, J. W. Rawlins and D. A. Savin, *ACS Appl. Mater. Interfaces*, 2013, **5**, 11004–11013.
87 A. Oesterreicher, J. Wiener, M. Roth, A. Moser, R. Gmeiner, M. Edler, G. Pinter and T. Griesser, *Polym. Chem.*, 2016, **7**, 5169–5180.
88 P. Esfandiari, S. C. Ligon, J. J. Lagref, R. Frantz, Z. Cherkaoui and R. Liska, *J. Polym. Sci., Part A: Polym. Chem.*, 2013, **51**, 4261–4266.
89 M. Podgórski, E. Becka, M. Claudino, A. Flores, P. K. Shah, J. W. Stansbury and C. N. Bowman, *Dent. Mater.*, 2015, **31**, 1263–1270.
90 M. Podgórski, C. Wang, Y. Yuan, D. Konetski, I. Smalyukh and C. N. Bowman, *Chem. Mater.*, 2016, **28**, 5102–5109.
91 C. Gorsche, K. Seidler, P. Knaack, P. Dorfinger, T. Koch, J. Stampfl, N. Moszner and R. Liska, *Polym. Chem.*, 2016, **7**, 2009–2014.
92 T. F. Scott, A. D. Schneider, W. D. Cook and C. N. Bowman, *Science*, 2005, **308**, 1615–1617.
93 S. C. Ligon-Auer, M. Schwentenwein, C. Gorsche, J. Stampfl and R. Liska, *Polym. Chem.*, 2016, **7**, 257–286.
94 J. C. Kloxin, F. T. Scott and N. C. Bowman, *Macromolecules*, 2009, **42**, 2551–2556.
95 T. F. Scott, R. B. Draughon and C. N. Bowman, *Adv. Mater.*, 2006, **18**, 2128–2132.

96 H. Y. Park, C. J. Kloxin, T. F. Scott and C. N. Bowman, *Macromolecules*, 2010, **43**, 10188–10190.
97 H. Y. Park, C. J. Kloxin, T. F. Scott and C. N. Bowman, *Dent. Mater.*, 2010, **26**, 1010–1016.
98 C. Gorsche, T. Koch, N. Moszner and R. Liska, *Polym. Chem.*, 2015, **6**, 2038–2047.
99 C. Gorsche, M. Griesser, G. Gescheidt, N. Moszner and R. Liska, *Macromolecules*, 2014, **47**, 7327–7336.
100 H. Algamaiah, N. Silikas and D. C. Watts, *Dent. Mater.*, 2021, **37**, 559–567.
101 T. Roshan, E. Rizzardo, J. Chiefari, J. Krstina, G. Moad, A. Postma and S. H. Thang, *Macromolecules*, 2000, **33**, 243–245.
102 H. Y. Park, C. J. Kloxin, M. F. Fordney and C. N. Bowman, *Dent. Mater.*, 2012, **28**, 888–893.
103 M. Oguri, Y. Yoshida, K. Yoshihara, T. Miyauchi, Y. Nakamura, S. Shimoda, M. Hanabusa, Y. Momoi and B. Van Meerbeek, *Acta Biomater.*, 2012, **8**, 1928–1934.
104 F. Morlet-Savary, J. E. Klee, F. Pfefferkorn, J. P. Fouassier and J. Lalevée, *Macromol. Chem. Phys.*, 2015, **216**, 2161–2170.
105 N. Ilie and R. Hickel, *Dent. Mater. J.*, 2008, **27**, 221–228.
106 L. Roedel, V. Bednarzig, R. Belli, A. Petschelt, U. Lohbauer and J. Zorzin, *Clin. Oral Invest.*, 2017, **21**, 1735–1741.
107 C. S. Pfeifer, J. L. Ferracane, R. L. Sakaguchi and R. R. Braga, *Am. J. Dent.*, 2009, **22**, 206–2010.
108 A. Kowalska, J. Sokolowski, T. Gozdek, M. Krasowski, K. Kopacz and K. Bociong, *Polymers*, 2021, **13**, 3972.
109 W. M. Palin, M. A. Hadis, J. G. Leprince, G. Leloup, L. Boland, G. J. P. Fleming, G. Krastl and D. C. Watts, *Dent. Mater.*, 2014, **30**, 507–516.
110 R. L. Sakaguchi, B. D. Wiltbank and N. C. Shah, *Dent. Mater.*, 2004, **20**, 388–396.
111 T. G. Oberholzer, S. R. Grobler, C. H. Pameijer and R. J. Rossouw, *Meas. Sci. Technol.*, 2002, **13**, 78–83.
112 R. Mulder, S. R. Grobler and Y. I. Osman, *Oral Biol. Dent.*, 2013, **1**, 1.
113 X. Wang, G. Huyang, S. V. Palagummi, X. Liu, D. Skrtic, C. Beauchamp, R. Bowen and J. Sun, *Dent. Mater.*, 2018, **34**, 228–237.
114 A. J. de Gee, C. L. Davidson and A. Smith, *J. Dent.*, 1981, **9**, 36–42.
115 X. Wang, G. Huyang, S. V. Palagummi, X. Liu, D. Skrtic, C. Beauchamp, R. Bowen and J. Sun, *Dent. Mater.*, 2018, **34**, 228–237.
116 H. L. Lee, M. L. Swartz and F. F. Smith, *J. Dent. Res.*, 1969, **48**, 526–535.
117 A. J. de Gee, A. J. Feilzer and C. L. Davidson, *Dent. Mater.*, 1993, **9**, 11–14.
118 D. U. Shah and P. J. Schubel, *Polym. Test.*, 2010, **29**, 629–639.
119 A. Nejadebrahim, M. Ebrahimi, X. Allonas, C. Croutxé-Barghorn, C. Ley and B. Métral, *RSC Adv.*, 2019, **9**, 39709–39720.
120 M. Topa-Skwarczyńska, A. Świeży, D. Krok, K. Starzak, P. Niezgoda, B. Oksiuta, W. Wałczyk and J. Ortyl, *Int. J. Mol. Sci.*, 2022, **23**, 10470.
121 W. D. Cook, M. Forrest and A. A. Goodwin, *Dent. Mater.*, 1999, **15**, 447–449.
122 R. L. Sakaguchi, C. T. Sasik, M. A. Bunczak and W. H. Douglas, *J. Dent.*, 1991, **19**, 312–316.
123 G. Q. D. M. Monteiro, M. A. J. R. Montes, T. V. Rolim, C. C. B. de Oliveira Mota, B. D. B. C. Kyotoku, A. S. L. Gomes and A. Z. De Freitas, *Dent. Mater.*, 2011, **27**, e176–e185.
124 ISO – ISO 17304:2013 – Dentistry—Polymerization shrinkage: Method for determination of polymerization shrinkage of polymer-based restorative materials, **https://www.iso.org/standard/59772.html**, (accessed 25 January 2023).
125 S. Luo, F. Liu and J. He, *J. Mech. Behav. Biomed. Mater.*, 2019, **94**, 222–228.
126 J. He, S. Garoushi, P. K. Vallittu and L. Lassila, *Acta Biomater. Odontol. Scand.*, 2018, **4**, 30–37.
127 M. Zhao, Y. Geng, S. Fan, X. Yao, M. Zhu and Y. Zhang, *Compos. Sci. Technol.*, 2021, **213**, 108902.
128 D. C. Watts and A. J. Cash, *A. J. Dent. Mater.*, 1991, **7**, 281–287.
129 F. A. P. Rizzante, J. A. Duque, M. A. H. Duarte, R. F. L. Mondelli, G. Mendonça and S. K. Ishikiriama, *Dent. Mater. J.*, 2019, **38**, 403–410.
130 J. Y. Li, A. Lau and A. S. L. Fok, *J. Zhejiang Univ., Sci., A*, 2013, **14**, 1–10.
131 R. Danso, B. Hoedebecke, K. Whang, S. Sarrami, A. Johnston, S. Flipse, N. Wong and H. R. Rawls, *Dent. Mater.*, 2018, **34**, 1459–1465.
132 J. Li, P. Thakur and A. S. L. Fok, *J. Visualized Exp.*, 2014, 1–9.
133 S. Luo, F. Liu, B. Yu and J. He, *J. Biomater. Sci. Polym. Ed.*, 2019, **30**, 137–149.
134 T. A. T. Canellas, A. de Almeida Neves, I. K. dos Santos, A. R. P. de Rezende, C. E. Fellows and E. M. da Silva, *J. Mech. Behav. Biomed. Mater.*, 2019, **90**, 566–574.
135 C. E. Cuevas-Suárez, J. A. González-López, A. F. da Silva, E. Piva and A. M. Herrera-González, *J. Mech. Behav. Biomed. Mater.*, 2018, **87**, 148–154.
136 B. Pratap, R. K. Gupta, B. Bhardwaj and M. Nag, *Mater. Today: Proc.*, 2020, **33**, 2567–2569.